Nuclear Instruments and Methods in Physics Research A 770 (2015) 189–196

Contents lists available at ScienceDirect

Nuclear Instruments and Methods in Physics Research A

journal homepage: www.elsevier.com/locate/nima

The NUCLEON space experiment for direct high energy cosmic rays investigation in TeV–PeV energy range

E. Atkin [a], V. Bulatov [b], V. Dorokhov [b], N. Gorbunov [c], S. Filippov [b], V. Grebenyuk [c], D. Karmanov [d], I. Kovalev [d], I. Kudryashov [d], M. Merkin [d], A. Pakhomov [d], D. Podorozhny [d], D. Polkov [b], S. Porokhovoy [c], V. Shumikhin [a], L. Sveshnikova [d], A. Tkachenko [c], L. Tkachev [c], A. Turundaevskiy [d,*], O. Vasiliev [d], A. Voronin [d]

[a] National Research Nuclear University "MEPhI", Moscow 115409, Russia
[b] SDB Automatika, Ekaterinburg 620075, Russia
[c] Joint Institute for Nuclear Research, Dubna 141980, Russia
[d] Skobeltsyn Institute of Nuclear Physics, Moscow State University, Moscow 119991, Russia

ARTICLE INFO

Article history:
Received 30 April 2014
Received in revised form
24 September 2014
Accepted 28 September 2014
Available online 8 October 2014

Keywords:
High energy cosmic rays
Calorimeter
Energy measurements

ABSTRACT

The NUCLEON satellite experiment is designed to investigate directly, above the atmosphere, the energy spectra of cosmic-ray nuclei and the chemical composition from 100 GeV to 1000 TeV as well as the cosmic-ray electron spectrum from 20 GeV to 3 TeV. NUCLEON is planned to be launched in 2014. This mission is aimed at clarifying the essential details of cosmic-ray origin in this energy interval: number and types of sources, identification of actual nearby sources, and the investigation of the mechanisms responsible for the knee. Specific features of the NUCLEON instrument are relatively small thickness and small weight. A special method of energy determination by the silicon tracker was developed for this case. In this paper we describe a design of the instrument and the results of accelerator beam tests in terms of charge and energy resolution. The overall evidences of the capability of the apparatus to achieve the declared aims are also presented.

1. Introduction

The "knee" energy range 10^{14}–10^{16} eV is a crucial region for the understanding of the cosmic-ray (CR) origin, acceleration and propagation in our galaxy. It is important to obtain more data in this energy range with elemental CR resolution. The "knee" area is interesting for astrophysics.

Currently available data are not enough for the creation of a final adequate interpretation of "knee". Indirect methods using registration of atmospheric showers with energy levels higher than 10^{14} eV are dependent on interaction models. There are different hypotheses explaining the phenomenon of the "knee". Direct measurements of the chemical composition of cosmic rays are necessary to solve this problem.

Another important problem is the secondary to primary nuclei ratio at high energies (> 100 GeV/nucleon). It is connected with a study of mechanisms of the cosmic-ray propagation in the galaxy.

The cosmic-ray anisotropy is a fundamental problem too. For example, the anisotropy can depend on stochastic character of supernova explosions [1].

Thus new experiments over a wide charge and energy range are needed. It would help to test existing theoretical conceptions and would become a basis for further studies in this very important field of knowledge. Long-duration balloon experiments like ATIC [2–4], TRACER [5], and CREAM [6] have begun to solve the above-mentioned problems. But a real solution to the problems would be possible only with a long-term large aperture satellite experiment. Some important results were obtained by the PAMELA satellite [7,8], AMS02 [9,10], and Fermi-LAT [11], currently taking data.

The high energy electrons spectrum depends on actual nearby sources of cosmic rays. For high energy electrons the dominant energy loss mechanism is the synchrotron radiation when traversing through the galactic magnetic fields. Therefore, the propagation distance for ultrarelativistic electrons is limited.

There are sufficient differences in experimental results obtained by different experiments [2,3,7,8,10,11] at high energies. New experimental data are necessary.

The main difficulty of high energy cosmic-ray direct investigations is to lift primary particles energy detectors outside the Earth's

* Corresponding author.
E-mail address: torn@front.ru (A. Turundaevskiy).

http://dx.doi.org/10.1016/j.nima.2014.09.079
0168-9002/

atmosphere. Now the most universal energy measurements technique is ionisation calorimeter. This method is reliable but a calorimeter needs a heavy absorber to register high energy showers. Weight restrictions limit the application of ionisation calorimeters for cosmic-ray investigation on board of satellites at energies >100 TeV.

A new energy measurement method KLEM (Kinematic Lightweight Energy Meter) was proposed [12]. The primary energy is reconstructed by registration of spatial density of the secondary particles. The particles are generated by the first hadronic inelastic interaction in a carbon target. Then additional particles are produced in thin tungsten converter by electromagnetic and hadronic interactions. The main difference between the proposed KLEM method and ionisation calorimeters is that the KLEM technique does not need heavy absorbers for the shower measurement. Thus it is possible to design relatively light cosmic rays' detectors with a large geometric factor.

The NUCLEON experiment was proposed [12–21]. The basic concept of the experiment is to design a scientific device with a relatively small weight (300–400 kg) and volume (<1 m^3). The device must provide information about some of the most fundamental questions in astroparticle physics today. The main aim of the experiment is to investigate cosmic-ray nuclei energy spectra from 100 GeV to 1000 TeV and electrons spectrum from 20 GeV to 3 TeV by direct methods.

The NUCLEON experiment does not need a special satellite. The device will be exposed on board the serial Russian satellite by means of an application of weight reserve. Such weight reserve exists on some serial satellites. This approach should reduce the costs of the experiment.

2. Experimental technique

The main idea is to use a new experimental method KLEM in the NUCLEON project for the CR energy measurement to achieve above-mentioned aims.

The proposed technique can be used over a wide range of energies (10^{11}–10^{16} eV) and gives an energy resolution of 70% or better according to simulation results [15,18,21].

The kinematical method for the determination of the primary particle energy was proposed by Castagnoli [22] and gives large errors between 100% and 200%. To overcome this problem, a combined method was proposed. On the one hand, it is based on the measurements of spatial density of not only charged secondaries but also neutral ones. On the other hand we propose a measuring technique at the data processing stage that allows an increased contribution of faster secondaries to energy determination and eliminates that of slower ones. The principal scheme is the following.

A primary particle interacts in the thin carbon target where secondary photons (originated via decays of π^0) and charged particles are produced. The converter, that is a set of thin tungsten layers, converts almost all secondary photons to electron–positron pairs. These new electrons can radiate more photons that in turn produce additional electrons at the initial part of the shower. There is an initial part of a shower in the converter. The most energetic photons produce more secondary charged particles. Presence of the converter results in a significant multiplication of charged particles after the converter. Energy dependence of total number of charged particles after the converter is steeper than analogous dependence for a primary interaction multiplicity. Generally the energy dependence of total number of charged particles changes from logarithmic to linear by increase of thickness of the converter up to the shower maximum. The real converter is significantly thinner. The most energetic secondaries have minimal values of the polar angles θ. Thus the most significant multiplication of charged particles is for large pseudo-rapidity. We made the entire procedure more sensitive to primary energy (E) measurement.

In the development of the data processing technique we propose to use the S-estimator for the energy determination:

$$S=\sum_{i=1}^{N}\eta_i^2 \tag{1}$$

where summation is over all N-secondaries detected after the converter, $\eta_i=-\ln \mathrm{tg}\,\theta_i/2\approx-\ln(2r_i/H)$, and r_i is a distance from the shower axis for all position-sensitive detector layers located after the converter, and H is a distance from the interaction point in the target. For the real apparatus we apply H determined as distance from the middle of target to the detector layer. The systematic uncertainty is small in comparison with physical fluctuations. For example the value of $\ln^2(2H/x)$ is equal to 48.4 for the middle region of target ($H=255$ mm) and 45.4 for the low boundary of target ($H=204$ mm). Thus the maximal systematic deviation is near 6%. The direct simulation shows that the rms deviation of reconstructed energy (see below) increased from 70% (for true interaction point) to 70.2%. On the one hand S-estimator characterises the distribution of secondaries on emission angles, being sensitive to the Lorentz-factor of the primary particle, and on the other hand S is proportional to the multiplicity of secondaries produced in the target and multiplied in the converter. The contribution of slow neutrals is eliminated by the squaring of η. The simulation showed a simple semi-empirical power law energy dependence for S [13].

The perpendicular projections x_i and y_i can be used instead of a distance r_i. It allows exploiting microstrip silicon detectors for spatial measurements.

The microstrip detectors can register many charged particles per strip. The signal is proportional to the strip ionisation or the number of single-charged particles. Thus S-estimator is defined as

$$S=\Sigma I_k \ln^2(2H/x_k) \tag{2}$$

where x_k is distance between the shower axis and the strip k and I_k is a signal in the strip k. Thus the $S(E)$-estimator is the sum in quadrature of parameters $\ln(H/2x_k)$ closed to pseudo-rapidities. The estimator depends on the angular distribution of secondaries. The number of secondaries with minimal angles is more sensitive to the Lorentz factor of primary particle than the total multiplicity. The squaring increases contribution of these particles. The simple semi-empirical power law $\langle S(E)\rangle\sim E^{0.7-0.8}$ dependence of the energy per nucleon was obtained. The above-mentioned squaring and multiplication of secondaries in the converter make energy dependence steeper than for multiplicity in the first interaction. For incident nucleus with mass number A only a part of the nucleons – N_w – interacts with the target carbon nucleus. Therefore the multiplicity of secondaries is not proportional to A but the angular distribution of secondaries is similar to the distribution for one proton. The $\langle S(E)\rangle$ dependence is similar for different types of primary nuclei in a wide range. A detailed simulation was performed. The new method permits the reconstruction of primary energy spectra that may have some peculiarities such as deviations from simple power law. On this basis, the NUCLEON device for primary cosmic-ray measurements in satellite investigations was constructed and tested on accelerator beams.

The application of different kinematical estimators is discussed in Ref. [23]. The NUCLEON design allows different approaches to data processing.

3. NUCLEON design

The NUCLEON device will be placed on board the RESURS-P satellite. The spacecraft will be launched on a Sun-synchronous orbit with inclination 97.276° and a middle height above Earth's surface of 475 ± 5 km. The effective geometric factor is more than 0.2 m^2 sr for the KLEM system and near 0.1 m^2 sr for the calorimeter. The surface area of the device is equal to 0.25 m^2. The

charge measurement system must provide resolution better than 0.3 charge unit. The NUCLEON device must permit separation of the electromagnetic and hadronic CR components at the rejection level better than 10^{-3} for the events in a calorimeter aperture. The total weight of the device is about 375 kg. Power consumption is less than 175 W. The planned exposition time is more than 5 years.

Science objectives and detection technique determine the detector design. The general composition of the NUCLEON apparatus (a) and its disposition on board the RESURS-P satellite (b) are presented in Fig. 1. The NUCLEON apparatus includes the charge measurement system consisting of the 4 pad silicon detectors layers (1), the KLEM energy measurement system consisting of the carbon target (2) and the silicon microstrip detectors interleaved with thin tungsten layers (3), the trigger system consisting of the 6 scintillator layers (5) and the calorimeter (4). Silicon detectors consist of unified ladders.

The charge detector system is designed for precision measurement of the primary particle charge and consists of four thin detector layers of 1.5×1.5 cm^2 silicon pads. Each readout channel is used for the two pads to decrease number of channels. Signals of two pads from different parts of detector are summed. Probability of simultaneous registration of two particles is negligible. Charge measurement readout chips CR-1 have a dynamic range $\sim$1000 mip.

The energy measurement system consists of silicon microstrip layers with perpendicular orientation. The pitch of microstrips is equal to 484 μm. The microstrips must also be used to determine a secondary particle shower axis for the primary particle trajectory measurement. The spatial distribution of signals is approximated by Gaussian curves for every layer to determine the shower axis coordinates. The distance H from the interaction point to microstrip layer is determined as distance from the middle of target to the layer divided by $\cos(\theta_x)$ or $\cos(\theta_y)$. The angles θ_x and θ_y are projections of shower axis polar angle.

The tungsten layers convert almost all secondary gamma-quanta to electron–positron pairs. This significantly increases the number of secondary particles and therefore improves the accuracy of a primary particle energy determination. Every strip is connected to its own readout channel. The perpendicular strip orientation makes it possible to perform analysis for each x and y direction independently and improve the primary particle energy resolution.

There are six layers of the scintillator detectors with thickness of 0.75 cm in the trigger system. They are aimed to generate necessary trigger signals for the KLEM system. Each of the trigger planes consists of 16 scintillator strips. The light signals from the strips are collected by the wavelength shifting fibres (WLS) to photomultiplier tubes (PMT).

The satellite restrictions did not allow the creation of a full-aperture calorimeter; thus its transversal size was limited to 250×250 mm^2 and a weight of $\sim$26 kg.

The ionisation calorimeter (MIC) has a thickness of 12 radiation lengths. Hence, the installation's full length, including the target and the energy measurement system, equals 15.2 radiation lengths. The equivalent thickness of the carbon target is equal to 0.23 proton interaction length. The calorimeter's base consists of 6 tungsten plane absorbers of two radiation lengths each (Fig. 1). The 6 layers of 300 μm silicon microstrip detectors, positioned between the tungsten planes on textolite leaders, are sensitive elements of the calorimeter. Strip stepping is roughly 1 mm.

The calorimeter must register the secondary particles shower after the KLEM energy measurement system. The calorimeter must be used to select and to measure the electromagnetic component (electrons, positrons, gamma) from the total CR flux. Also the calorimeter allows measurement of the hadronic component energy for onboard calibration of the KLEM method.

Some NUCLEON device units were designed and tested [19–21].

4. Testing an integrated circuit for read-out signals

The Geant4 Monte-Carlo simulation of showers from different particles (protons, nuclei) with energies from 10^3 to 10^4 GeV gives the energy deposit in one strip up to 25,000 mip. Hence, to achieve the experiment's minimal physical goals, the readout system must have a dynamic range of 25,000 and a *signal-to-noise* ratio (SNR) of at least 2.

A classical charge sensitive amplifier (CSA) chip with linear transfer function with such requirements would have a too high power consumption, which would exceed the available NUCLEON power limit.

For the NUCLEON experiment an application-specific integrated circuit (ASIC) was designed to read out data from the detectors [24,25]. This 32-channel chip was developed by the MEPHI ASIC lab, manufactured via Europractice by 0.35 μm CMOS process of AMIS (OnSemi). A chip demonstrator board was designed and tested at the silicon detector lab of SINP MSU, confirming a dynamic range of up to 30,000 at an SNR of 2.5 and a power consumption of 3.5 mW/channel.

An increase of the dynamic range in this chip was achieved by using a polygonal transfer function. It was implemented by using an auxiliary capacitor inserted into the CSA's negative feedback. This capacitor switches on automatically when the input signal reaches a specific level, and lowers the CSA's gain. As a result, the transfer characteristic of the chip consists of two straight segments with different angles of inclination (Fig. 2).

5. Beam test of charge measurement system

The NUCLEON device and its different systems were tested by accelerator beams, including the charge measurement system tests by ions beams. The tests were performed at the SPS accelerator in CERN in 2005 [20] and 2013. A beam of indium nuclei with an energy

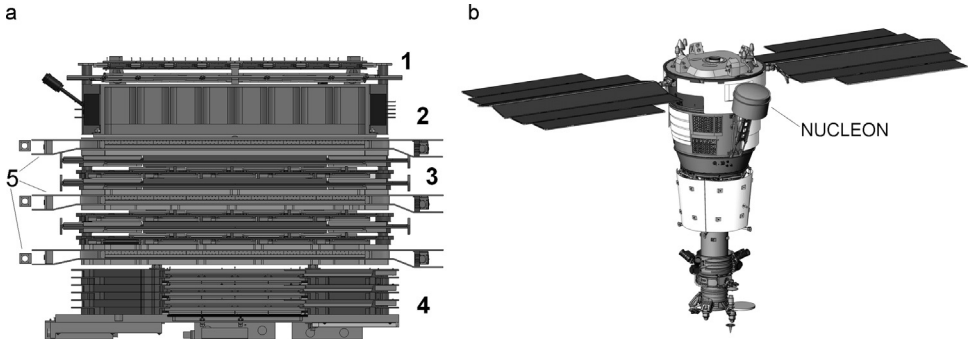

Fig. 1. The NUCLEON device general configuration (left) and the RESURS-P satellite (right). The NUCLEON apparatus includes the charge measurement system consisting of the 4 pad silicon detectors layers (1), the KLEM energy measurement system consisting of the carbon target (2) and the silicon microstrip detectors divided by thin tungsten layers (3), the trigger system consisting of the 6 scintillator layers (5) and the calorimeter (4).

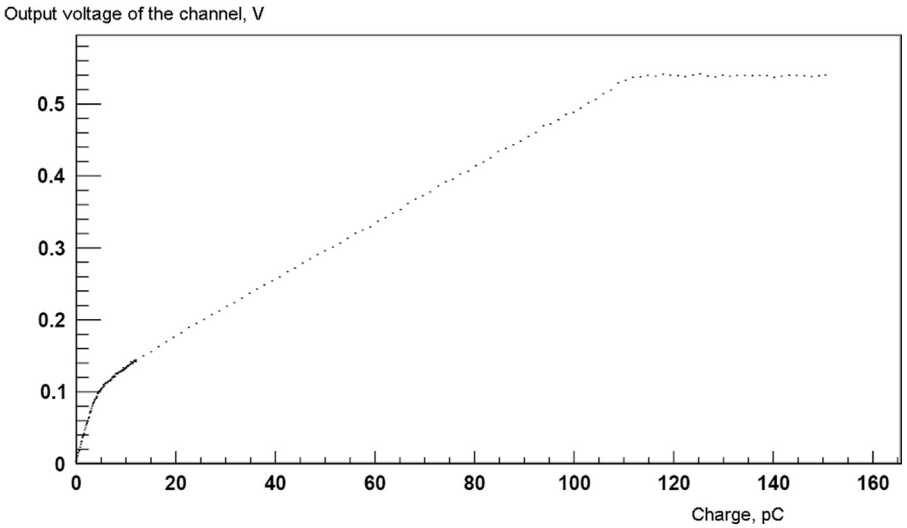

Fig. 2. The transfer function of the chip.

of ~158 GeV/nucleon was directed toward a 4-cm-thick beryllium target. The secondary charged particles and nuclear fragments were then separated according to their rigidity by means of a magnetic deflection system. In the experiment, particles with rigidities of 157.65, 315.5, 319.0, and 339.56 GeV/Z (Z is the nuclear charge) were selected. Since the energy per nucleon was constant for all the nuclei produced by fragmentation of indium, each value of the magnetic rigidity corresponded to a particular value of the ratio of the mass number to the charge A/Z (1.000, 2.000, 2.023, and 2.154). It is evident that the first value corresponds only to protons; the second to deuterium, ^{4}He, ^{6}Li, ^{10}B, ^{12}C, etc.; the third to ^{87}Tc or ^{89}Ru (unstable isotopes with a very short lifetime); and the fourth to ^{28}Al and ^{56}Fe.

The system for determining the charge consists of four layers of silicon detectors composed of separate pads. Information on the incident particle charge is collected from each array independently of the others, which guarantees a higher accuracy of measurements than that achieved by a single array. Various algorithms of particle charge reconstruction were worked out. The calibration curves were obtained for all channels.

The charge spectra of the four detectors were matched using the rank statistics method [20]. For each recorded event four charges were measured by the four detectors and arranged in ascending order (regardless of the detector to which a particular charge corresponded). The next step was to determine the charge that is second in magnitude, and this value was used as the estimate for the charge. It should be noted that the rank statistics method provides better results than mere averaging of values, since fluctuations of the ionisation losses have a sharply asymmetrical form as opposed to the standard distribution of errors. This method decreases errors caused by nuclear spallation and secondary particles generation in the detector.

The procedure for measuring the charges of various nuclei using four arrays of pad silicon detectors allowed determining the particle charges. Comparison of the charge distributions obtained in the test experiment on the accelerator to the results of the simulation has demonstrated consistency.

These results lead to the conclusion that the technique for measuring the charge in the NUCLEON experiment, together with the equipment intended for this experiment, will offer a chance to measure the charge composition of high-energy CR with an accuracy of 0.2–0.3 charge unit, which is sufficient both for discriminating separate CR components and for studying the abundance of secondary nuclei in CR flux at high energies. The total grammage of the charge measurement system is about 1.5 g/cm^2. Thus probability of spallation is sufficiently small even for iron nuclei.

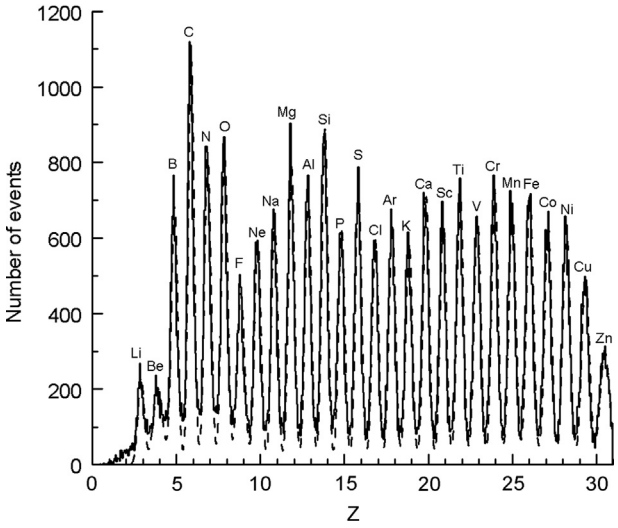

Fig. 3. Beam test charge distribution (solid line) in comparison with the multi-Gaussian approximation (dashed line).

In 2013 a NUCLEON test accumulated more than 400,000 nuclear events with a parameter $A/Z=2.1$ and some variants of trigger requirements. The objectives of this test were to confirm the possibility of separation of the different nuclei in the charge measurement system of the NUCLEON apparatus.

In the charge measurement system there are peaks from different nuclei up to $Z=30$ with reasonable separation. The results of measurements are shown in Fig. 3 (solid line) in comparison with a multi-Gaussian fit (dashed line). Light nuclei were not investigated, so A/Z-parameter value 2.1 and a rather hard electronic trigger was used. This is the reason why the proton (deuteron) and helium peaks are not seen in Fig. 3 and lithium/beryllium peaks are suppressed too. Also the channel gain in electronics of the charge measurement system is not perfectly linear; the real signal from the heavy nuclei ($Z>25$) is higher than it should be from the standard dependence of the signal on the square of nuclear charge. This information will be very useful for our real experiment.

6. Beam tests of energy measurement system

The main energy measurement system of the NUCLEON experiment is based on the KLEM method. The practical applicability of

the proposed technique was estimated using the results of the simulation employing the GEANT 3.21 [26] software package complemented by the QGSJET [27] nuclear interaction generator to describe high-energy hadron–nucleus and nucleus–nucleus interactions.

Different spectrometer structures were investigated to choose an optimal design of a detector operating according to the KLEM technique in a 100–10,000 GeV energy range.

For simulation and experimental data analysis an S-estimator according to the Eq. (2) is applied.

Simulation showed that the energy dependence obeys power law $S(E)$ over a wide range of energies for nuclei with $Z=1$–30 and the power law index 0.74–0.82. The energy resolution is defined as the rms deviation of reconstructed value of E. The resolution is rather poor (~70%). However in measuring the descending CR spectrum, it is considerably better (~50%). The reconstructed energy distribution is convolution of the distribution for fixed primary energy with spectral function. Simulation showed a decrease of rms deviation for asymmetric reconstructed energy distribution. Therefore the KLEM method can be used to measure the CR power spectrum in the desired energy range.

This method provides a means to create an experimental set-up with a relatively low mass and for high CR flux that opens prospects for developing an orbital spectrometer with a long exposure time and carrying our investigations of CRs over a wide energy range with a unified technique. Careful tests of the KLEM method with NUCLEON prototypes were performed at the hadron 100–350 GeV beams of the SPS accelerator at CERN [21]. The procedure for reconstructing the particle energy uses the theoretical calibration dependence of parameter $S(E)$. Based on the simulation data, the calibration dependence $\langle S(E)\rangle$ estimator of energy was plotted and the power law index was found to be 0.75.

For the 350 GeV pion beam the mean energy measured using the KLEM technique is equal to 334 GeV, and the rms deviation is equal to 0.79 of mean value. For the simulation results mean reconstructed energy is equal to 350 GeV and rms deviation/mean value ratio is equal to 0.78 for the NUCLEON prototype.

The NUCLEON flight model was tested in 2012 on pion and electron beams of the SPS accelerator at CERN. Pion data were obtained for 150 and 350 GeV. Shower axes coordinates were determined by microstrip detectors' signals. The S values were calculated for every selected event. Energy dependence $S(E)$ is obtained and shown in Fig. 4 for a pion beam of 2013 (squares) and the previous 2008 tests (circles). The point at 200 GeV is significantly out of fitted line due to a different trigger selection.

The normalised distributions of the reconstructed energy for primary pions with energies of 150 (thin line) and 350 GeV (thick line) are shown in Fig. 5. The rms deviation to primary energy ratio is equal to 0.53 for 150 GeV and 0.63 for 350 GeV. The asymmetry of distributions is determined by the asymmetry of multiplicity distributions for hadron interactions. The resolution is better than for the prototype because of the strict trigger selection.

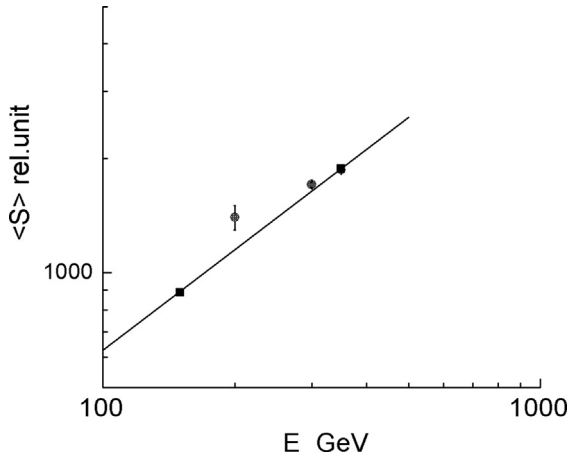

Fig. 4. The $\langle S(E)\rangle$ calibration energy dependence for pion beams in 2012 (squares) and previous 2008 tests (circles).

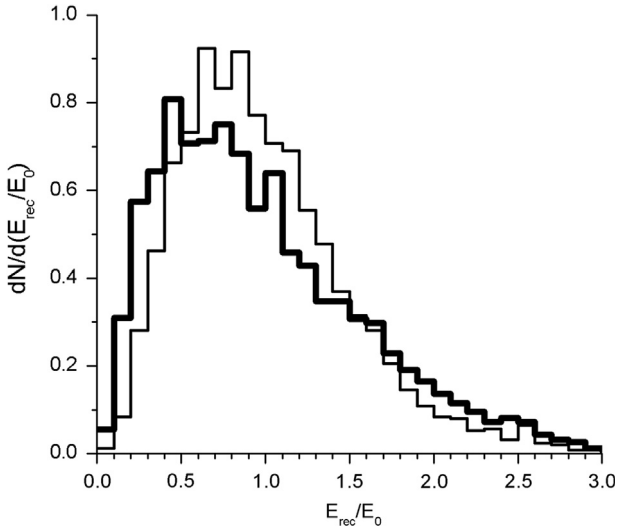

Fig. 5. Normalised reconstructed energy distributions for pion beams of 150 GeV (thin line) and 350 GeV (thick line).

7. Calibrations of the NUCLEON calorimeter

Energy deposit in the calorimeter can be determined by reconstruction of cascade curves. To reconstruct primary energies for electrons, correction coefficients determined by simulation were used. Calibration curves are presented in Fig. 6.

Two approaches of energy reconstruction were applied to consider leakage of energy out of the calorimeter. In the first case the cascade curve was approximated (circles, dotted line), and in the second one the full energy deposit was multiplied by a constant coefficient (squares, solid line). Parameters were determined from simulation results. Correction coefficients were determined by comparison of mean real and reconstructed energies.

Reconstructed energy distributions for 100, 150 and 200 GeV electrons are shown in Fig. 7 (thick solid line) in comparison with simulation results (dashed line). The experimental distributions are wider than simulated ones. Possibly this difference is caused by different amplification coefficients of readout chips and hadronic contamination of beams. The Gaussian fits for experiment (thin solid line) and simulation (dotted line) are presented too. The calorimeter energy measurements resolution is better than 10% for electromagnetic events. The rms deviations are equal to 7.5%, 9.3%, 6.2% for experiment and 4.5%, 4.0%, 3.7% for simulation.

Trajectories of hadrons, electrons and gamma-quanta can be reconstructed by means of microstrip and scintillator detectors data. An example of transverse spatial distribution of the calorimeter first detector plane is presented in Fig. 8a. The angular distribution of reconstructed track directions based on all detectors data is presented in Fig. 8b for the 300 GeV pion beam. The RMS of this angular distribution is equal to 0.9° that is sufficient for anisotropy CR investigations.

Besides the KLEM methodic flight calibration, the MIC performs the CR electron component energy measurement. Energy

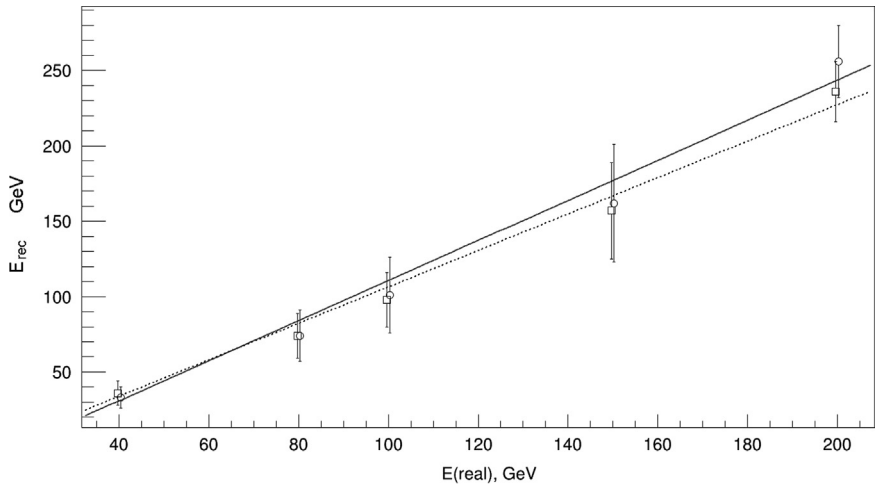

Fig. 6. The calorimeter calibration curves. Cascade curve approximation (circles, dotted line) and full energy deposit (squares, solid line).

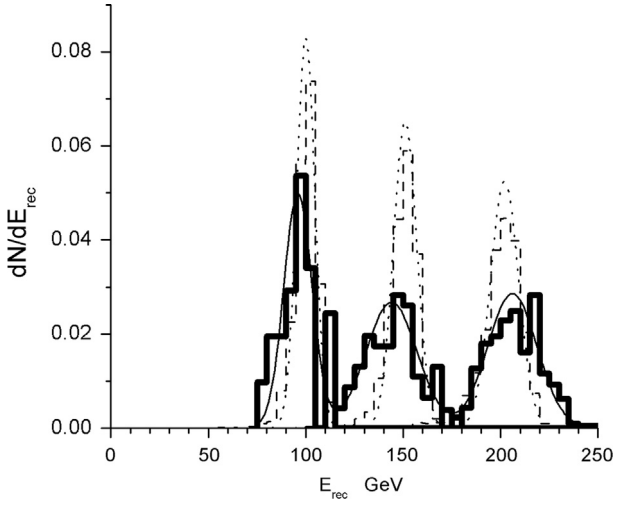

Fig. 7. Calorimeter reconstructed energy distributions for 100, 150 and 200 GeV electron beams (solid line) in comparison with simulation results (dashed line) and Gaussian fits for experiment (thin solid line) and simulation (dotted line).

resolution of the apparatus for the electrons is roughly 15% for energies from 10^3 to 10^4 GeV. Multi-variable analysis based on energetic and topologic differences between electromagnetic and nuclear cascades allows separation of the electrons from the hadrons.

8. Separation of electron and hadron events

Hadron and electromagnetic events can be separated by the shape of the cascade in the NUCLEON device. Two similar approaches were developed for such separation, both based on a similar set of variables but using different methods for their analysis.

The spatial resolution of microstrip detectors is equal to ~0.5 mm for the KLEM energy measurement system and ~1 mm for the calorimeter.

Microstrip detectors data can be applied to reconstruct longitudinal and transverse cascade ionisation distributions and describe a shower by a set of parameters.

Longitudinal cascade ionisation distribution is well described by the empiric formula $dE/dt = E_0 b[(bt)^{a-1}e^{-bt}]/\Gamma(a)$ [28]; variables from this parametrisation are used in one of the analysis methods. These parameters' values are different, naturally, for electromagnetic and hadron showers. The a parameter determines the shape of initial part of showers. The b parameter determines the energy absorption at the tail of showers. The gamma function $\Gamma(a)$ is used for normalisation.

The hadron cascade cross-section is wider than the electromagnetic one for different reasons. The longitudinal cascade distribution depends on the presence of charged hadrons and electrons generated by secondary interactions.

The cascade process gives rise to a self-similar pattern that can be described by shower fractal dimension [29]. Fractal dimension is a ratio providing a statistical index of complexity comparing how details in a pattern change with the scale at which it is measured. Fractal dimension can be applied to describe different objects [30]. The fractal dimensions of hadron and electromagnetic showers are different due to difference of physical processes.

The set of parameters was determined for the selection of the hadron–electron showers at the detector simulation. In the first method eight parameters are chosen to describe the main shower characteristics by a small number of variables.

The following list of shower parameters is used: (i) i, the number of the calorimeter-detector layer where the energy deposition is maximal; (ii) $T_m = E_i/\sum_k E_k$, the ratio of the energy deposition in the ith layer to the total energy deposition in the calorimeter; (iii) $T_l = \ln(\sum_k E_k)$, the natural logarithm of the total energy deposition in the calorimeter; (iv) $T_c = E_{ia}/Ei$, the ratio of the maximal signal in a strip to the sum of the signals in the i layer; (v) m, the number of near-axis strips in the ith layer where half of the layer ionisation occurs; (vi) T_{12}, a parameter that characterises the fractal character of the shower curve in the calorimeter, $T_{12} = \sum_{k=1}^{5}\left(1+(E_{k+1}-E_k)^2\right)/\sum_{k=1}^{3}\left(4+(E_{2k}-E_{2k-1})^2\right)$ (this parameter characterises the change in the shower-curve length (in terms of the shower-depth and energy-deposition coordinates) in response to a change in the scale); (vii) A_q; and (viii) B_q.

The last two parameters are obtained upon approximating the initial shower-curve segment (within the upper part of the NUCLEON setup) by an exponential function: $\ln E_k = kA_q + B_q$ [31].

In the second method the three parameters of cascade curve parametrisation (a, b, E_0) are used.

Both methods use multivariate analysis (MVA). The difference between the methods is that the first uses artificial neural networks exclusively, while the second uses a MVA toolkit (TMVA), which allows application of different minimisation algorithms. Boosted decision tree (BDT) algorithm was chosen because it provided the

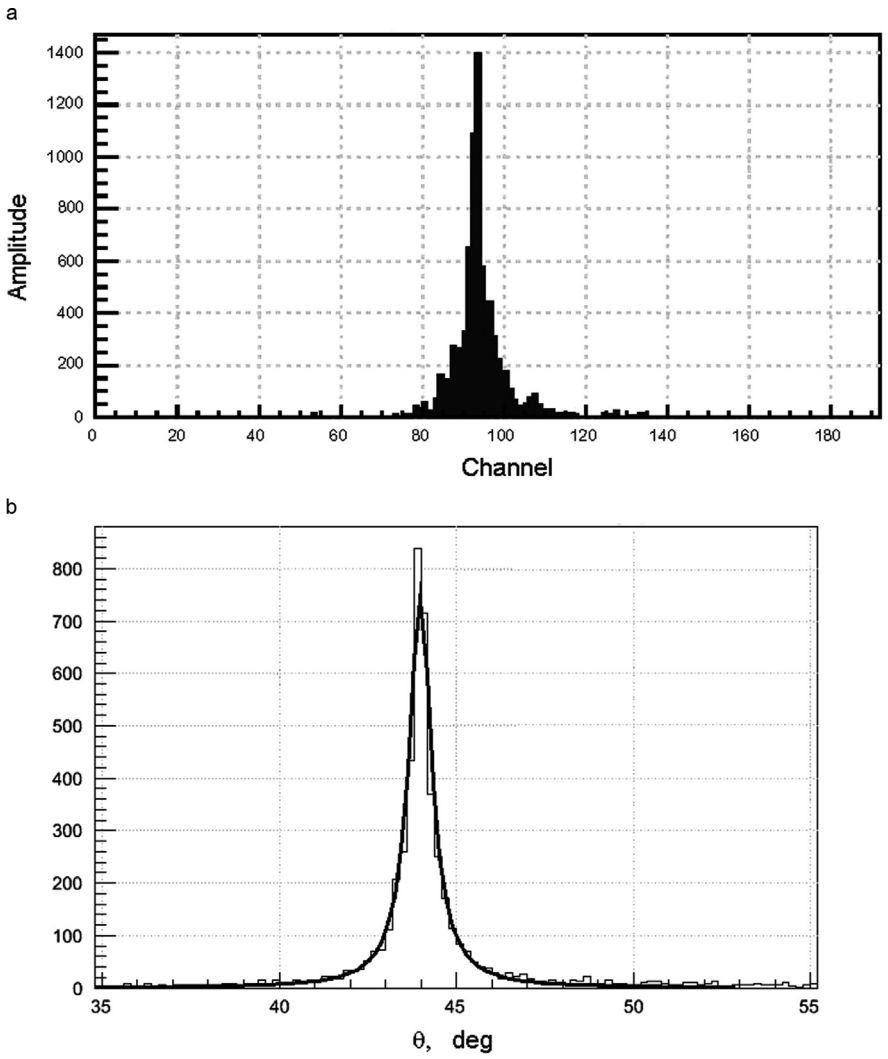

Fig. 8. An example of transverse spatial distribution of the calorimeter first detector plane (a) and the angular distribution of reconstructed track directions based on all detectors (b). Angular distribution is fitted by the Gaussian function.

most effective separation. After testing these methods with Monte-Carlo simulation data, they were applied to the test beam data.

Obtained results can be estimated by two characteristics:

1) Background efficiency is suppression ratio for hadronic events. It is the ratio of quantity of hadrons registered as electrons to real quantity of electrons.
2) Signal efficiency is electromagnetic events registration probability for set point of background efficiency.

The dependence of the first method error probability on the neural network generalised parameter is shown in Fig. 9 for electrons (squares) and pions (circles). The network generalised parameter is equal to 0 if the particle is reliably identified as an electron and to 1 if the particle is reliably identified as a pion. For real events, values of the generalised parameter are between 0 and 1. Different levels of this parameter can be used to distinguish particles.

The background efficiency dependences on signal efficiency, obtained using the second method, are presented in Fig. 10.

The background efficiency is better than 10^{-3} for signal efficiency ~80%. This background efficiency is obtained for equal energy deposit in the calorimeter. The energy deposit for hadrons is determined by energy of secondary photons produced by the first interaction. This energy is, on the average, equal to 0.3 of total energy of pions or 0.2 of total energy of protons. Thus electrons with energy E can be contaminated by protons with energy $E/0.2$. By comparing the electron flux at 1 TeV [11] and the proton flux at 5 TeV [3] we estimate that the proton contamination corresponding to a background efficiency 10^{-3} is ~1%. These two independent analysis methods showed that the NUCLEON space experiment can achieve a hadron–electron separation sufficient to accurately reconstruct the CR electron spectrum.

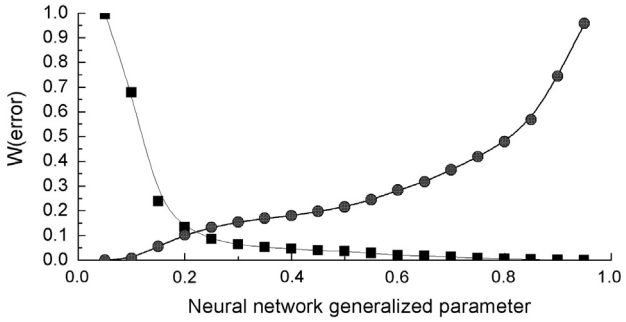

Fig. 9. Error probability dependences on neural network generalised parameter. Probability of electron registration as pion is marked by squares and probability of pion registration as electron is marked by circles.

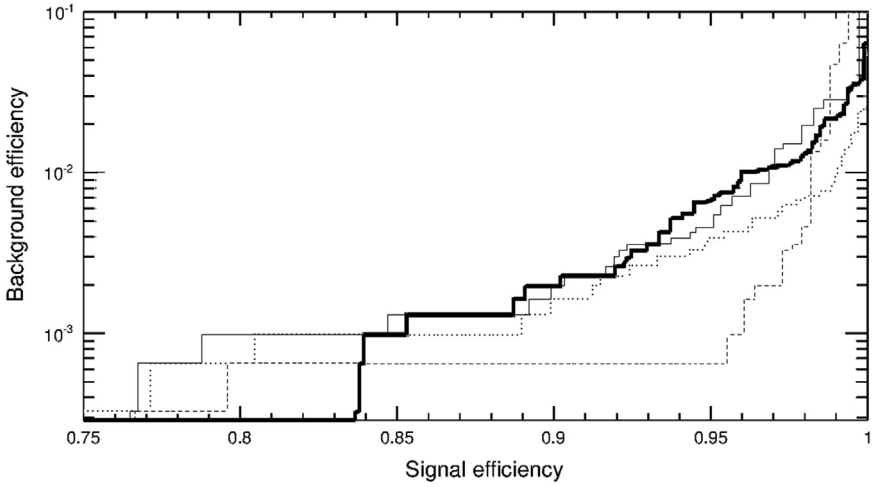

Fig. 10. Background efficiency vs signal efficiency in beam tests. The BDT analysis is applied. π vs 150 GeV e^- is dotted line, π vs 100 GeV e^- is dashed line, π vs all e^- is thin solid line, π vs 200 GeV e^- is thick solid line.

9. Conclusions

The NUCLEON device was designed and tested. The expected performance is confirmed by simulation and beam test results. All scientific objectives are achievable. The launch of the satellite is planned for 2014.

Acknowledgements

The reported study was supported by the Supercomputing Center of Lomonosov Moscow State University [32].

References

[1] A.D. Erlykin, A.W. Wolfendale, Astroparticle Physics 25 (2006) 183.
[2] J. Chang, J.H. Adams, H.S. Ahn, et al., Nature 456 (2008) 362.
[3] A.D. Panov, V.I. Zatsepin, N.V. Sokolskaya, et al., Astrophysics and Space Sciences Transactions 7 (2011) 119.
[4] H.S. Ahn, E.S. Seo, J.H. Adams, et al., Advances in Space Research 37 (2006) 1950.
[5] P. Boyle, D. Muller, M. Ave, et al., Advances in Space Research 42 (2008) 409.
[6] E.S. Seo, H.S. Ahn, J.J. Beatty, et al., Advances in Space Research 33 (2004) 1777.
[7] W. Menn, O. Adriani, G. Barbarino, et al., Advances in Space Research 51 (2013) 209.
[8] O. Adriani, G.C. Barbarino, G.A. Bazilevskaya, et al., Physical Review Letters 106 (2011) 201101.
[9] M. Aguilar, G. Alberti, B. Alpat, et al., Physical Review Letters 110 (2013) 141102.
[10] R. Battiston, Physics of the Dark Universe 4 (2014) 6.
[11] M. Ackermann, M. Ajello, W.B. Atwood, et al., Physical Review D 82 (2010) 092004.
[12] J. Adams, G. Bashindzhagyan, A. Chilingaryan, et al., AIP Conference Proceedings 504 (2000) 175.
[13] J. Adams, G. Bashindzhagyan, P. Bashindzhagyan, et al., Advances in Space Research 27 (2001) 829.
[14] N. Korotkova, D. Podorozhnyi, E. Postnikov, et al., Physics of Atomic Nuclei 65 (2002) 852.
[15] E. Postnikov, G. Bashindzhagyan, N. Korotkova, et al., Izvestiya Akademii Nauk SSSR Seriya Fizicheskaya 66 (2002) 1634.
[16] D. Podorozhnyi, E. Postnikov, L. Sveshnikova, A. Turundaevsky, Physics of Atomic Nuclei 68 (2005) 50.
[17] G. Bashindzhagyan, A. Voronin, S. Golubkov, et al., Instruments and Experimental Techniques 48 (2005) 32.
[18] D. Podorozhnyi, V. Bulatov, N. Baranova, et al., Bulletin of the Russian Academy of Sciences: Physics 71 (2007) 500.
[19] G. Voronin, V. Grebenyuk, D. Karmanov, et al., Instruments and Experimental Techniques 50 (2007) 176.
[20] G. Voronin, V. Grebenyuk, D. Karmanov, et al., Instruments and Experimental Techniques 50 (2007) 187.
[21] V. Bulatov, A. Vlasov, N. Gorbunov, et al., Instruments and Experimental Techniques 53 (2010) 29.
[22] C. Castagnoli, et al., Nuovo Cimento 10 (1953) 1239.
[23] K. Batkov, G. Bigongiari, P. Maestro, et al., Astroparticle Physics 35 (2011) 50.
[24] E.V. Atkin, Yu.A. Volkov, A.G. Voronin, et al., Instruments and Experimental Techniques 55 (2012) 456.
[25] E. Atkin, A. Klyuev, et al., Russian Microelectronics 40 (2011) 52.
[26] GEANT User's Guide. CERN DD/EE/83/1. Geneva, 1983.
[27] N.N. Kalmykov, S.S. Ostapchenko, A.I. Pavlov, Nuclear Physics B (Proceedings Supplements) 52 (1997) 17.
[28] G. Grindhammer, S. Peters, The parameterized simulation of electroma gnetic showers in homogeneous and sampling calorimeters. (arXiv:hep-ex/0001020).
[29] Manqi Ruan, Journal of Physics: Conference Series 490 (2014) 012227.
[30] B.B. Mandelbrot, Journal of Statistical Physics 34 (1983) 895.
[31] O. Vasilyev, D. Karmanov, I. Kovalyov, et al., Physics of Atomic Nuclei 77 (2014) 587.
[32] V. Sadovnichy, A. Tikhonravov, VI. Voevodin, V. Opanasenko, "Lomonosov": Supercomputing at Moscow State University, Contemporary High Performance Computing: From Petascale toward Exascale (Chapman & Hall/CRC Computational Science), CRC Press, Boca Raton, USA (2013) 283–307.